

# Coordinate Activation of Maternal Protein Degradation during the Egg-to-Embryo Transition in *C. elegans*

Jason Pellettieri,<sup>1</sup> Valerie Reinke,<sup>2</sup>  
Stuart K. Kim,<sup>3</sup> and Geraldine Seydoux<sup>1,\*</sup>

<sup>1</sup>Department of Molecular Biology and Genetics  
Johns Hopkins University School of Medicine  
Baltimore, Maryland 21205

<sup>2</sup>Department of Genetics  
Yale University School of Medicine  
New Haven, Connecticut 06520

<sup>3</sup>Department of Developmental Biology and  
Department of Genetics  
Stanford University School of Medicine  
Stanford, California 94305

## Summary

The transition from egg to embryo occurs in the absence of transcription yet requires significant changes in gene activity. Here, we show that the *C. elegans* DYRK family kinase MBK-2 coordinates the degradation of several maternal proteins, and is essential for zygotes to complete cytokinesis and pattern the first embryonic axis. In *mbk-2* mutants, the meiosis-specific katanin subunits MEI-1 and MEI-2 persist during mitosis and the first mitotic division fails. *mbk-2* is also required for posterior enrichment of the germ plasm before the first cleavage, and degradation of germ plasm components in anterior cells after cleavage. MBK-2 distribution changes dramatically after fertilization during the meiotic divisions, and this change correlates with activation of *mbk-2*-dependent processes. We propose that MBK-2 functions as a temporal regulator of protein stability, and that coordinate activation of maternal protein degradation is one of the mechanisms that drives the transition from symmetric egg to patterned embryo.

## Introduction

Fertilization transforms a nondividing, mostly symmetric egg into a cleaving embryo that rapidly develops visible asymmetries. This transition occurs before mRNA transcription commences, and therefore any changes in gene expression must occur posttranscriptionally. Translational recruitment of maternal RNAs is a common mechanism to generate new proteins in maturing oocytes and newly fertilized zygotes. For example, in *Xenopus laevis*, oocyte maturation triggers phosphorylation of CPEB (cytoplasmic polyadenylation element binding protein), which in turn activates the polyadenylation and translation of several maternal RNAs (Mendez and Richter, 2001). In principle, coordinated degradation of maternal proteins could also drive the transition from oocyte to embryo. Examples of maternal protein degradation after fertilization have been reported (e.g., Suzumori et al., 2003), but whether these degradations are coordinately regulated and the extent to which they influence embryonic development is not known.

In *C. elegans*, fertilization triggers two major responses: transition from meiosis to mitosis and establishment of the first embryonic axis (anterior-posterior; A-P). The mechanisms that mediate these responses are still poorly understood, but protein degradation has been implicated in both. Immediately following fertilization, the maternal chromatin, which was arrested in prophase of meiosis I, completes the two meiotic divisions. The haploid maternal and paternal pronuclei undergo S phase, fuse with each other, and complete mitosis on a spindle elaborated by the sperm asters. Transition from the short, barrel-shaped meiotic spindles to the large mitotic spindle requires downregulation of MEI-1 and MEI-2 (Dow and Mains, 1998; Srayko et al., 2000). MEI-1 and MEI-2 are homologs of the p60 and p80 subunits of a heterodimeric microtubule-severing complex in sea urchins called katanin (McNally and Vale, 1993). They associate with the meiotic spindle and are required for the meiotic divisions, but if allowed to persist after meiosis, interfere with mitotic spindle dynamics (Dow and Mains, 1998; Kurz et al., 2002; Srayko et al., 2000). Downregulation of MEI-1/2 depends on recognition by an E3 ubiquitin ligase, containing the cullin CUL-3 and the novel substrate recruitment factor MEL-26 (L. Pintard et al., submitted). The mechanism that activates MEI-1/2 degradation after meiosis is not known.

A-P polarity is initiated after meiosis by interactions between the sperm asters and the actin-rich cortex (Lyzak et al., 2002). The PAR and MEX polarity regulators divide the zygote into nonoverlapping anterior and posterior domains, eventually causing the segregation of a specialized cytoplasm (germ plasm) to a single posterior blastomere that will form the germline. Segregation of the germ plasm is a complex, multistep process, which depends on at least two independent mechanisms: posterior enrichment in the zygote before the first cleavage, and degradation of a subset of germ plasm proteins (CCCH proteins) in anterior cells after cleavage (Reese et al., 2000). Recent studies have shown that degradation of CCCH proteins depends on recognition by an E3 ubiquitin ligase, containing the cullin CUL-2 and the substrate recognition factor ZIF-1 (DeRenzo et al., 2003). The mechanisms that mediate posterior enrichment of the germ plasm in the zygote and activate CCCH protein degradation in anterior cells are not known.

In this study, we report that the MEI-1/2 and CCCH protein degradation pathways are regulated by a common kinase called MBK-2. MBK-2 also regulates germ plasm asymmetry in the zygote, implicating a common regulatory network for these processes. We propose that, like translational activation of maternal RNAs, coordinated degradation of maternal proteins is one of the mechanisms that drive the egg-to-embryo transition.

## Results

### Identification of *mbk-2*

We identified *mbk-2* in an RNAi-based screen for genes required for posterior localization of PIE-1, a CCCH finger protein component of the germ plasm (Experimental

\*Correspondence: gseydoux@jhmi.edu

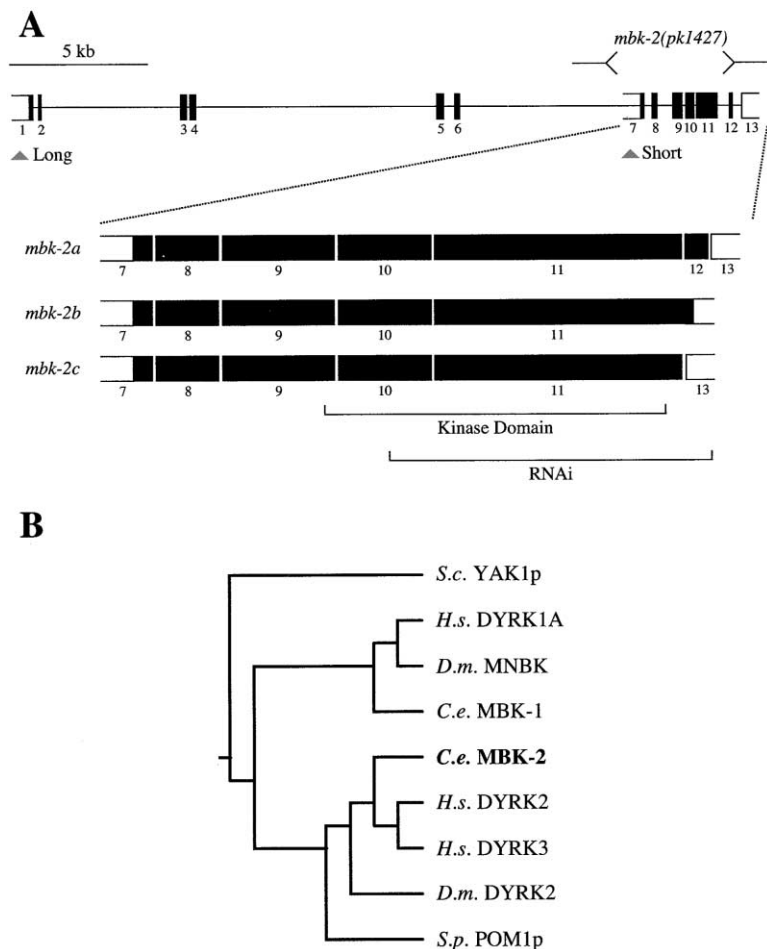


Figure 1. *mbk-2* Encodes a DYRK Family Protein Kinase

(A) EST alignments (<http://www.wormbase.org>) and sequencing of cDNAs (our unpublished results) reveal multiple transcripts at the *mbk-2* locus. Exons (boxes) and introns (lines) are drawn to scale, except for the 5'- and 3'-most exons whose exact 5' and 3' ends, respectively, are not known. Coding regions in exons are shaded in black. Exons 1 and 7 are alternative 5' exons that initiate "long" and "short" transcripts, respectively. In long transcripts, exon 6 is spliced directly to exon 8, bypassing exon 7. Alternative splicing of exons 11, 12, and 13 gives rise to three different 3' ends. For clarity, only the short transcripts (*mbk-2a*, *b*, and *c*) are shown. (B) Clustal W tree of MBK-2 and a subset of DYRK family kinases. The dendrogram was generated using the predicted kinase domains for each protein. *S.c.*, *Saccharomyces cerevisiae*; *H.s.*, *Homo sapiens*; *D.m.*, *Drosophila melanogaster*; *C.e.*, *Caenorhabditis elegans*; *S.p.*, *Schizosaccharomyces pombe*. See also Raich et al., 2003.

Procedures). The *mbk-2* locus encodes multiple mRNAs, including "long" and "short" transcripts initiated from alternative 5' exons (Figure 1A). RNAi targeting of the long transcripts resulted in ~15% embryonic lethality but did not disrupt PIE-1 localization (data not shown). In contrast, RNAi against a region present in all transcripts resulted in 100% embryonic lethality and PIE-1 mislocalization. Identical embryonic phenotypes were seen in the progeny of hermaphrodites homozygous for *pk1427*, a deletion that removes most of the region included in the short transcripts (Raich et al., 2003). A transgene corresponding to one of the shorter transcripts (*mbk-2c*; Figure 1A) was able to rescue the embryonic lethality of *pk1427* (Experimental Procedures), indicating that *mbk-2c* is sufficient for the embryonic functions of *mbk-2*.

*mbk-2c* encodes a predicted 502 amino acid protein, MBK-2, which belongs to the emerging family of dual-specificity Yak1-related kinases (DYRKs). These kinases share sequence homology primarily in their kinase domain and in a 10–50 amino acid region immediately upstream of the catalytic domain (Becker and Joost, 1999). Several members of this protein family have been shown to phosphorylate both serine/threonine and tyrosine residues in vitro (Becker et al., 1998; Kentrup et al., 1996). DYRKs are found in species ranging from yeast to human, including YAK1 in *S. cerevisiae* (Garrett and Broach, 1989), *minibrain* and DYRK2 in *Drosophila* (Tejedor et al., 1995), and DYRK1-4 in humans (Becker and

Joost, 1999). There are two DYRK family members in *C. elegans*, *mbk-1* and *mbk-2* (*minibrain-kinases*; Raich et al., 2003). Clustal W analysis of the kinase domains indicate that MBK-2 is most related to human DYRK2 and DYRK3, *Drosophila* DYRK2 (Becker and Joost, 1999), and *S. pombe* Pom1p (Bahler and Pringle, 1998; Figure 1B; see Discussion).

#### *mbk-2* Zygotes Exhibit Defects in Microtubule-Dependent Processes

Embryos derived from *mbk-2(pk1427)* hermaphrodites or hermaphrodites fed bacteria expressing *mbk-2* dsRNA (hereafter referred to as *mbk-2(pk1427)* embryos and *mbk-2(RNAi)* embryos, respectively) arrest development at the one-cell stage with multiple nuclei (Figure 2L). *mbk-2* embryos complete the meiotic divisions normally (Experimental Procedures), but begin to deviate from wild-type after formation of the pronuclei. Examination of live *mbk-2(pk1427)* and *mbk-2(RNAi)* zygotes by time-lapse microscopy revealed defects in microtubule-dependent processes. After meiosis, the maternal pronucleus migrates toward the paternal pronucleus and associated centrosomes at the posterior end of the zygote (Figures 2A and 2B; see Supplemental Movie 1 at <http://www.developmentalcell.com/cgi/content/full/5/3/451/DC1>). The pronuclei/centrosome complex migrates back toward the middle of the zygote (centration) and rotates (Figures 2B and 2C), so that the first mitotic

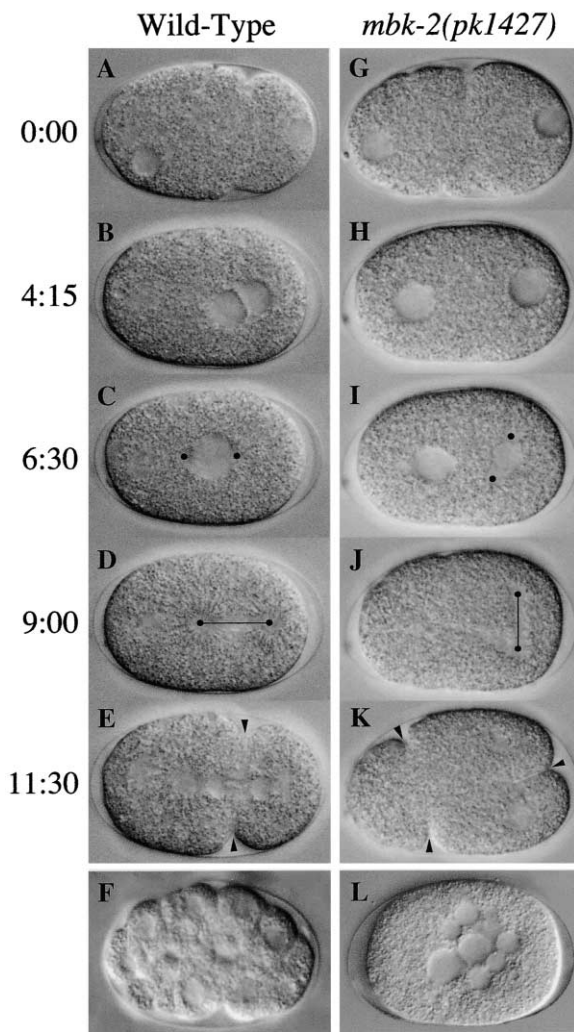


Figure 2. *mbk-2* Embryos Exhibit Defects in Microtubule-Dependent Processes

Images from time-lapse recordings of a wild-type zygote ([A–E]; Supplemental Movie 1) and an *mbk-2(pk1427)* zygote ([G–K]; Supplemental Movie 6). The time (min:s) at which each exposure was taken is indicated. Anterior is to the left and posterior is to the right in this and all subsequent figures. Black circles highlight the centrosomes, straight lines indicate the mitotic spindle, and arrowheads point to cleavage furrows.

(A and G) Pronuclear formation.

(B and H) Pronuclear meeting/migration.

(C and I) Late prophase of the first mitosis. Note that in this *mbk-2(pk1427)* zygote, pronuclear meeting and alignment of the spindle have failed.

(D and J) Anaphase.

(E and K) Cytokinesis onset.

(F and L) Representative embryos after multiple rounds of mitosis. *mbk-2(pk1427)* zygotes continue to cycle mitotically without completing cytokinesis.

spindle aligns along the long axis of the zygote (A–P axis; Figures 2C and 2D). In *mbk-2* zygotes, migration of the maternal pronucleus is delayed and rotation of the mitotic spindle often fails (Figures 2H–2J; Supplemental Movies 2–6). The severity of these defects varies considerably. For example, among nine *mbk-2(pk1427)* embryos examined by time-lapse microscopy, pronuclear

migration occurred normally in two embryos (e.g., Supplemental Movie 5), was delayed in five embryos (e.g., Supplemental Movie 6), and failed entirely in two embryos (e.g., Supplemental Movie 2; Figures 2G–2I). Similarly, the spindle aligned properly along the A–P axis in two embryos (e.g., Supplemental Movie 5), aligned initially but then became misaligned in two embryos (e.g., Supplemental Movie 3), and remained transverse to the A–P axis in five embryos (e.g., Supplemental Movie 6; Figure 2J).

Cleavage furrows were formed in all *mbk-2(pk1427)* and *mbk-2(RNAi)* embryos examined ( $n = 19$ ; Figure 2K), but in most cases retracted before completing cytokinesis (e.g., Supplemental Movie 4). Ectopic furrows were also observed in embryos with misaligned mitotic spindles (17/17; Figure 2K, arrowheads). Other actin-dependent processes, including pseudocleavage and cytoplasmic flow, appeared unaffected (Experimental Procedures). Cell cycle progression also proceeded normally, with nuclei undergoing several rounds of division in the absence of cytokinesis (e.g., Supplemental Movie 4).

To analyze the spindle defects of *mbk-2* mutants in greater detail, we made time-lapse recordings of embryos expressing a GFP: $\beta$ -Tubulin fusion (Strome et al., 2001; Figures 3A–3H; Supplemental Movies 7 and 8). As in wild-type, all five *mbk-2(RNAi)* embryos examined developed two prominent microtubule organizing centers around the male pronucleus and assembled a bipolar spindle upon entry into mitosis (Figures 3A and 3E). Defects in spindle morphology were first detected at the onset of anaphase. In wild-type embryos, the spindle began to elongate at this stage (Figures 3B and 3C; Supplemental Movie 7); in contrast in *mbk-2(RNAi)* zygotes, the spindle first decreased in length before elongating (5/5 embryos examined; Figures 3F and 3G; Supplemental Movie 8; Supplemental Figure S1). Microtubule density at the midzone appeared higher in *mbk-2(RNAi)* embryos, resulting in a prominent midbody remnant that persisted into cytokinesis (Figure 3H, arrow). Staining of endogenous tubulin with an anti-tubulin antibody confirmed these results (data not shown). In some cases, the spindle remnant appeared to block ingress of the cleavage furrow, raising the possibility that the *mbk-2* cytokinesis defects are secondary to spindle defects.

We also observed chromosome dynamics in wild-type and *mbk-2(RNAi)* embryos using a GFP:Histone H2B fusion (Praitis et al., 2001; Figures 3I and 3J; Supplemental Movies 9 and 10). As in wild-type, chromosomes began to condense during pronuclear migration and eventually congressed to form a metaphase plate in all five *mbk-2(RNAi)* embryos examined (Supplemental Movie 10). During anaphase, however, the chromosomal masses failed to fully separate in 4/5 embryos and remained linked by an “anaphase bridge” that persisted through telophase (Figure 3J; Supplemental Movie 10).

#### *mbk-2* Is Required for MEI-1 and MEI-2 Degradation

The cell division defects of *mbk-2* zygotes are reminiscent of those seen in *mei-26* and *rfl-1* mutants, which fail to degrade MEI-1 and MEI-2 before mitosis (Dow and Mains, 1998; Kurz et al., 2002). To test whether

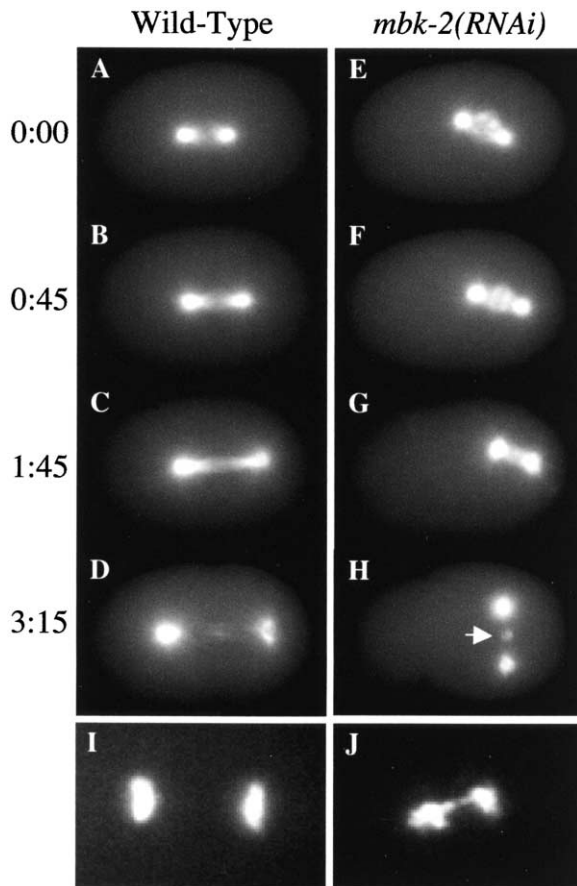


**Figure 3. Abnormal Microtubule and Chromatin Dynamics in *mbk-2* Zygotes Undergoing Mitosis**

Images from time-lapse recordings of a wild-type embryo ([A–D]; Supplemental Movie 7) and an *mbk-2(RNAi)* embryo ([E–H]; Supplemental Movie 8) expressing a GFP:β-Tubulin fusion protein. The time (min:s) at which each exposure was taken is indicated. (A and E) Metaphase. The *mbk-2(RNAi)* spindle is misaligned and exhibits a high density of midzone microtubules. (B and F) Metaphase-to-anaphase transition. (C and G) Anaphase. The *mbk-2(RNAi)* spindle has decreased in length. See Supplemental Figure S1 for a quantitative analysis of spindle length in *mbk-2(RNAi)* embryos. (D and H) Late anaphase/telophase. The *mbk-2(RNAi)* spindle is still shorter than wild-type and maintains a high density of microtubules in the middle of the spindle (arrow). (I and J) Images from time-lapse recordings of a wild-type embryo ([I]; Supplemental Movie 9) and an *mbk-2(RNAi)* embryo ([J]; Supplemental Movie 10) expressing a GFP:Histone H2B fusion. An “anaphase bridge” links the segregating chromosomes in the *mbk-2(RNAi)* zygote.

*mbk-2* is also required for MEI-1/2 degradation, we compared expression of a GFP:MEI-1 fusion (Pintard et al., 2003) in wild-type and *mbk-2(RNAi)* zygotes (Figures 4A–4D). In wild-type embryos, GFP:MEI-1 is readily detected on meiotic spindles but diminishes markedly before mitosis (Figures 4A and 4B). In contrast, we detected GFP:MEI-1 on both the meiotic and mitotic spindles of *mbk-2(RNAi)* embryos (Figures 4C and 4D). GFP:MEI-1 fluorescence eventually diminished, but only after the first mitotic division. Similar results were obtained for MEI-2 in immunostaining experiments (data

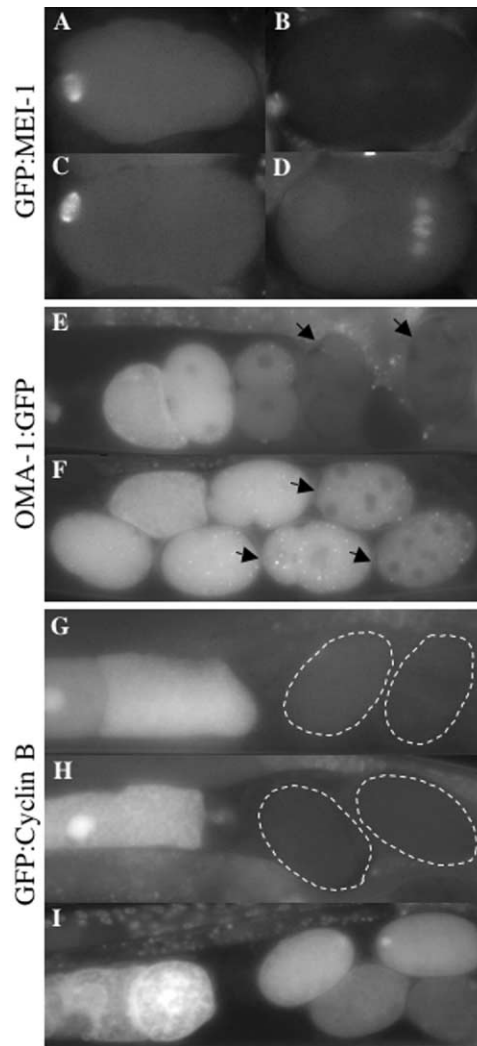


**Figure 4. *mbk-2* Is Required for the Degradation of Several Maternal Proteins**

(A–D) Wild-type (A and B) and *mbk-2(RNAi)* (C and D) zygotes expressing GFP:MEI-1. Zygotes in (A) and (C) are in meiosis; GFP:MEI-1 is on the meiotic spindle in both genotypes. Zygotes in (B) and (D) are in mitosis; GFP:MEI-1 is barely detectable in the wild-type zygote, but is abundant throughout the cytoplasm and on the spindle in the *mbk-2(RNAi)* zygote (11/13 *mbk-2(RNAi)* embryos examined during the first mitotic division had higher GFP:MEI-1 levels than wild-type). (E and F) Wild-type (E) and *mbk-2(RNAi)* (F) embryos expressing OMA-1:GFP. After two rounds of mitosis (embryos with arrows), OMA-1:GFP fluorescence is near background levels in wild-type, but still strong in *mbk-2(RNAi)*. (G–I) Wild-type (G), *mbk-2(RNAi)* (H), and *F49C12.8(RNAi)* (I) embryos expressing GFP:Cyclin B. *F49C12.8* encodes the *C. elegans* homolog of *S. cerevisiae* RPN7, a subunit of the proteasome. GFP:Cyclin B is present in oocytes (rectangular cells at the left) and is degraded shortly after fertilization in embryos (outlined) in both wild-type and *mbk-2(RNAi)*. In contrast, GFP:Cyclin B is maintained in *F49C12.8(RNAi)* embryos, which arrest immediately after fertilization in meiosis I (21/22 *F49C12.8(RNAi)* zygotes had GFP:Cyclin B compared to 0/11 *mbk-2(RNAi)* zygotes).

not shown). We conclude that *mbk-2* is required for timely turnover of MEI-1 and MEI-2 during the transition from meiosis to mitosis.

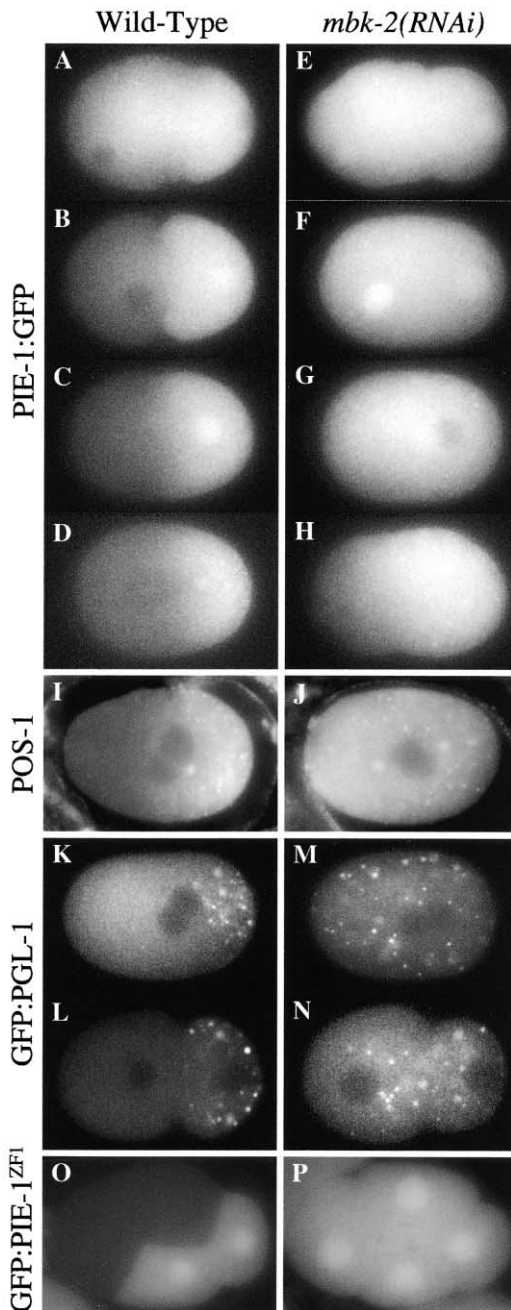


**Figure 5. *mbk-2* Is Required for Germ Plasm Asymmetry**  
 Images from time-lapse recordings of a wild-type embryo ([A–D]; Supplemental Movie 12) and an *mbk-2(RNAi)* embryo ([E–H]; Supplemental Movie 13) expressing PIE-1::GFP.  
 (A and E) Pronuclear formation.  
 (B and F) Pronuclear migration.  
 (C and G) Pronuclear meeting.  
 (D and H) Metaphase of the first mitosis.  
 PIE-1::GFP remained symmetric before mitosis in 0/8 wild-type embryos, 11/11 *mbk-2(RNAi)* embryos, and 4/5 *mbk-2(pk1427)* embryos (the odd embryo showed some posterior enrichment). PIE-1::GFP showed some posterior enrichment during mitosis in 16/16 *mbk-2* embryos.  
 (I and J) Fixed wild-type (I) and *mbk-2(RNAi)* (J) zygotes immunostained with anti-POS-1 antibody. POS-1 was symmetric in 22/22 *mbk-2(RNAi)* zygotes compared to 1/28 wild-type zygotes.  
 (K and M) Images from time-lapse recordings of wild-type ([K]; Sup-

The phenotypes of *rfl-1* mutants can be suppressed by depleting MEI-1 by RNAi (Kurz et al., 2002). We attempted similar experiments with *mbk-2(pk1427)* mutants. *mbk-2(pk1427)* embryos subjected to *mei-1(RNAi)* and/or *mei-2(RNAi)* had enlarged polar bodies and multiple maternal pronuclei, confirming that *mei-1/mei-2(RNAi)* was effective. These embryos, however, still failed to complete cytokinesis ( $n = 30$ ), and one *mbk-2(pk1427); mei-1(RNAi)/mei-2(RNAi)* embryo examined by time-lapse microscopy still failed to orient its mitotic spindle (Supplemental Movie 11). We conclude that *mbk-2* has other functions besides downregulation of MEI-1/2.

#### ***mbk-2* Is Required for the Degradation of OMA-1 but Not Cyclin B**

To explore whether *mbk-2* is required for the degradation of other factors besides MEI-1 and MEI-2, we examined the distribution of two other proteins known to be downregulated in early embryos. OMA-1 is a regulator of oocyte maturation, which accumulates in maturing oocytes and is degraded during early embryogenesis (Detwiler et al., 2001; Shimada et al., 2002). In wild-type, an OMA-1::GFP fusion (Lin, 2003) is readily detected in oocytes and one-cell embryos, but is rapidly turned over during the first cleavages (Figure 4E). In contrast, we found that OMA-1::GFP persisted through several rounds of mitosis in *mbk-2(RNAi)* embryos (Figure 4F). OMA-1::GFP levels eventually decreased, but with slower kinetics compared to wild-type. Failure to degrade OMA-1 was not due to a failure to complete cytokinesis, because OMA-1 degradation also failed in partially affected *mbk-2(RNAi)* embryos that complete several rounds of cytokinesis (Figure 4F; 29/31 multicellular embryos). We conclude that, in addition to MEI-1/2 degradation, *mbk-2* is also required for timely turnover of OMA-1 during the first mitotic divisions.

We also examined the distribution of Cyclin B, a cell cycle regulator, which accumulates in maturing oocytes and is rapidly degraded after fertilization during the meiotic divisions (E. Kipreos, personal communication; Figure 4G). We found that degradation of GFP::Cyclin B, although dependent on the proteasome (Figure 4I), was not dependent on *mbk-2*, even under the most stringent RNAi conditions (Figure 4H). This finding is consistent with the fact that *mbk-2(pk1427)* mutants proceed normally through the meiotic divisions and continue to cycle mitotically. We conclude that *mbk-2* is not generally required for protein degradation, but is essential for the timely degradation of a subset of maternal proteins.

plemental Movie 15) and *mbk-2(RNAi)* ([M]; Supplemental Movie 16) zygotes expressing GFP::PGL-1 to visualize P granules. GFP::PGL-1 remained symmetric in 0/4 wild-type embryos and 4/4 *mbk-2(RNAi)* embryos. Failure to localize P granules was also observed by immunofluorescence using a P granule antibody (data not shown). (L and N) Images of two-cell embryos expressing GFP::PGL-1 taken from time-lapse recordings of wild-type ([L]; Supplemental Movie 15) and *mbk-2(RNAi)* ([N]; Supplemental Movie 17). The *mbk-2(RNAi)* embryo was weakly affected by the RNAi treatment and underwent a normal asymmetric division, yet still failed to segregate P granules. (O and P) Wild-type (O) and *mbk-2(RNAi)* (P) four-cell embryos expressing GFP::PIE-1<sup>ZF1</sup>.

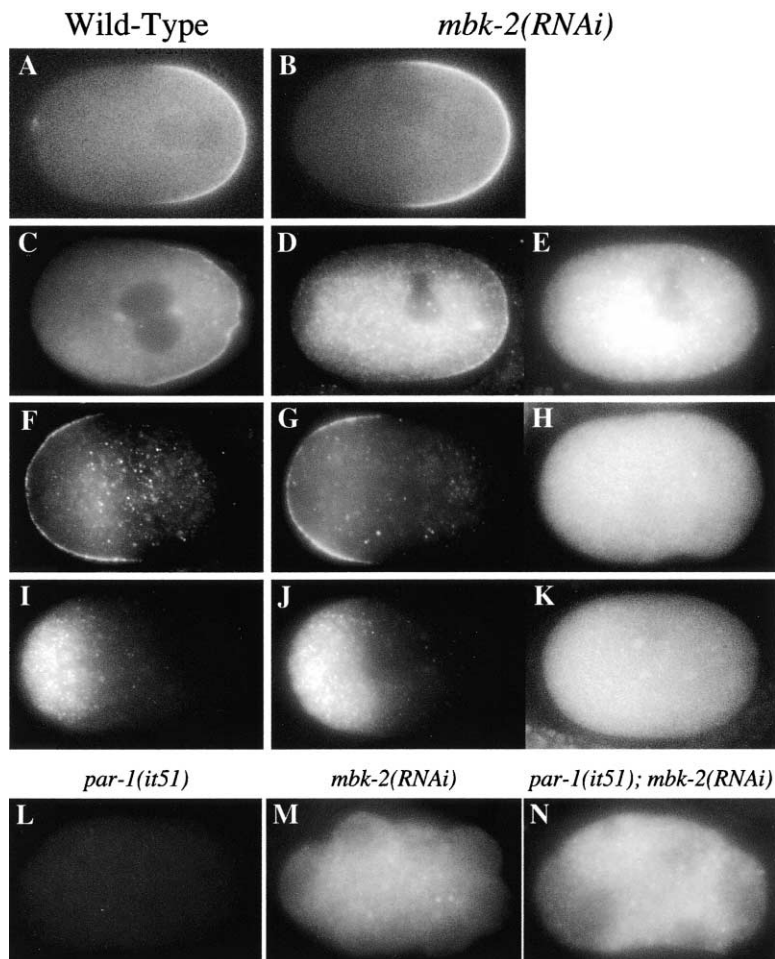


Figure 6. *mbk-2* Is Not Required for PAR or MEX-5 Asymmetry

All embryos are at the pronuclear meeting stage.

(A and B) Images from time-lapse recordings of wild-type (A; Supplemental Movie 18) and *mbk-2(RNAi)* (B; Supplemental Movie 19) zygotes expressing GFP:PAR-2. GFP:PAR-2 localized to the posterior cortex in 7/7 wild-type and 18/18 *mbk-2(RNAi)* zygotes examined by time-lapse recordings.

(C–K) Fixed zygotes immunostained for PAR-1 (C and D), PAR-3 (F and G), or MEX-5 (I and J). *mbk-2(RNAi)* embryos were simultaneously costained for PIE-1 (E, H, and K). PAR-1 localized to the posterior cortex in 13/13 wild-type and 23/24 *mbk-2(RNAi)* zygotes. PAR-3 localized to the anterior cortex in 6/6 wild-type and 25/28 *mbk-2(RNAi)* zygotes. MEX-5 localized to the anterior cytoplasm in 17/17 wild-type and 37/38 *mbk-2(RNAi)* zygotes. GFP:MEX-5 localized to the anterior as in wild-type in 3/3 *mbk-2(RNAi)* zygotes examined by time-lapse recordings (e.g., Supplemental Movie 21).

(L–N) Fixed embryos of the indicated genotypes immunostained for PIE-1. Eleven of 12 *mbk-2(RNAi)* and 10/11 *par-1(it51); mbk-2(RNAi)* four-cell and older embryos maintained high levels of PIE-1.

### *mbk-2* Is Required for Germ Plasm Asymmetry but Not for Initial Polarization of the Zygote

We originally isolated *mbk-2* on the basis of its PIE-1 mislocalization phenotype. To examine this phenotype in further detail, we performed time-lapse recordings of zygotes expressing a PIE-1:GFP fusion (Figures 5A–5H; Supplemental Movies 12–14). In wild-type embryos, PIE-1:GFP becomes enriched toward the posterior during pronuclear migration, and reaches maximum asymmetry by pronuclear meeting (Cuenca et al., 2003; Reese et al., 2000; Figures 5A–5C; Supplemental Movie 12). We found that *mbk-2* embryos failed to localize PIE-1 during pronuclear migration (Figures 5F and 5G; Supplemental Movies 13 and 14), and partially localized PIE-1 during mitosis (compare Figure 5H with Figure 5D). Immunofluorescence analysis of endogenous PIE-1 in fixed *mbk-2(RNAi)* embryos confirmed these results (Figures 6E, 6H, and 6K, and data not shown). We also examined the distribution of two other germ plasm components that segregate with PIE-1: the CCCH finger protein POS-1 (Tabara et al., 1999; Figures 5I and 5J), and ribonucleoprotein particles called P granules (Figures 5K–5N; Supplemental Movies 15 and 16). We found that POS-1 and P granules failed to segregate in *mbk-2(RNAi)* zygotes. In contrast to PIE-1, POS-1 and P granules never showed any asymmetry in *mbk-2(RNAi)*

zygotes, even during mitosis (Supplemental Movie 16 and data not shown).

Posterior localization of the germ plasm depends on the PAR and MEX proteins, which pattern the zygote along the A-P axis in response to a cue associated with the sperm asters (reviewed in Lyczak et al., 2002). The PDZ protein PAR-3 is enriched in the anterior cortex of the zygote (Etemad-Moghadam et al., 1995), whereas the RING finger protein PAR-2 and the serine/threonine kinase PAR-1 are enriched in the posterior cortex (Boyd et al., 1996; Guo and Kemphues, 1995). In the cytoplasm, the CCCH finger protein MEX-5 localizes to the anterior in a pattern reciprocal to that of PIE-1, POS-1, and P granules (Schubert et al., 2000). We found that establishment of anterior PAR-3 and MEX-5 domains and posterior PAR-1 and PAR-2 domains occurred normally in *mbk-2(RNAi)* embryos (Figure 6; Supplemental Movies 18–21). Double immunostaining experiments confirmed that these embryos do not localize PIE-1 before mitosis (Figures 6E, 6H, and 6K). We conclude that *mbk-2* is not required for initial polarization of the zygote, but is essential for the germ plasm to respond to PAR/MEX polarity cues.

During mitosis, PAR and MEX distributions began to deviate from wild-type in *mbk-2* mutants (Supplemental Movies 19 and 21; 13/18 *mbk-2(RNAi)* embryos mislocalized GFP:PAR-2, and 3/3 mislocalized GFP:MEX-5).

These defects appeared linked to the erratic spindle movements that arise during this period. Consistent with this hypothesis, GFP:PAR-2 was similarly mislocalized during mitosis in 6/6 embryos treated with the microtubule-depolymerizing drug nocodazole (Supplemental Movie 22). Nocodazole treatment, however, is not sufficient to disrupt germ plasm asymmetry, which is established before mitosis (Strome and Wood, 1983; 7/7 nocodazole-treated embryos localized PIE-1:GFP as in wild-type). Similarly, *mel-26* embryos, which like *mbk-2* mutants fail to degrade MEI-1 and do not orient their spindle properly, still segregated PIE-1 and P granules as in wild-type (16/18 *mel-26(RNAi)* embryos localized PIE-1:GFP like wild-type and 4/4 localized GFP:PGL-1 like wild-type). These observations suggest that the microtubule defects observed in *mbk-2* mutants, although sufficient to trigger the late PAR defects, are not sufficient to account for the lack of germ plasm asymmetry. To test this hypothesis further, we examined weakly affected *mbk-2(RNAi)* embryos, which orient their spindle, complete cytokinesis, and divide asymmetrically as in wild-type. These embryos still failed to localize PIE-1 and P granules (Figure 5N; Supplemental Movie 17; 16/16 asymmetric two-cell or four-cell *mbk-2(RNAi)* embryos had mislocalized PIE-1:GFP and 12/13 had mislocalized GFP:PGL-1). We conclude that the microtubule defects observed in *mbk-2* mutants are neither necessary nor sufficient to account for the defects in germ plasm segregation, suggesting that *mbk-2* regulates these two processes independently (see also Discussion).

#### ***mbk-2* Is Required for PIE-1 Degradation in Anterior Cells and Is Epistatic to *par-1***

After segregation in the zygote, the low levels of PIE-1 that remain in the anterior daughter cell are rapidly degraded. This degradation depends on the first CCCH finger of PIE-1 (Reese et al., 2000). A GFP:PIE-1<sup>ZF1</sup> fusion remains uniformly distributed in the zygote, but is rapidly degraded in anterior cells after cleavage, so that by the four-cell stage, it is present in only two posterior cells (Reese et al., 2000; Figure 5O). To test whether *mbk-2* is required for this process, we examined GFP:PIE-1<sup>ZF1</sup> in partially affected *mbk-2(RNAi)* embryos that successfully complete several rounds of division. These embryos failed to degrade GFP:PIE-1<sup>ZF1</sup> (n = 8; Figure 5P). We conclude that, in addition to regulating PIE-1 asymmetry in the zygote, *mbk-2* is also required to activate PIE-1 degradation in anterior cells.

PIE-1 degradation is blocked in posterior cells by PAR-1. In *par-1(it51)* embryos, PIE-1 is degraded in all cells (Reese et al., 2000; Tenenhaus et al., 1998; Figure 6L). We found that this ubiquitous degradation is dependent on MBK-2: *par-1(it51); mbk-2(RNAi)* “double mutants” maintain PIE-1 at high levels in all cells (Figure 6N). We conclude that *mbk-2* is epistatic to *par-1*, and is required for the ubiquitous degradation of PIE-1 that occurs in *par-1* mutants.

#### **MBK-2 Localization Is Dynamic**

To characterize the distribution of MBK-2 in oocytes and embryos, we constructed a GFP:MBK-2 fusion capable

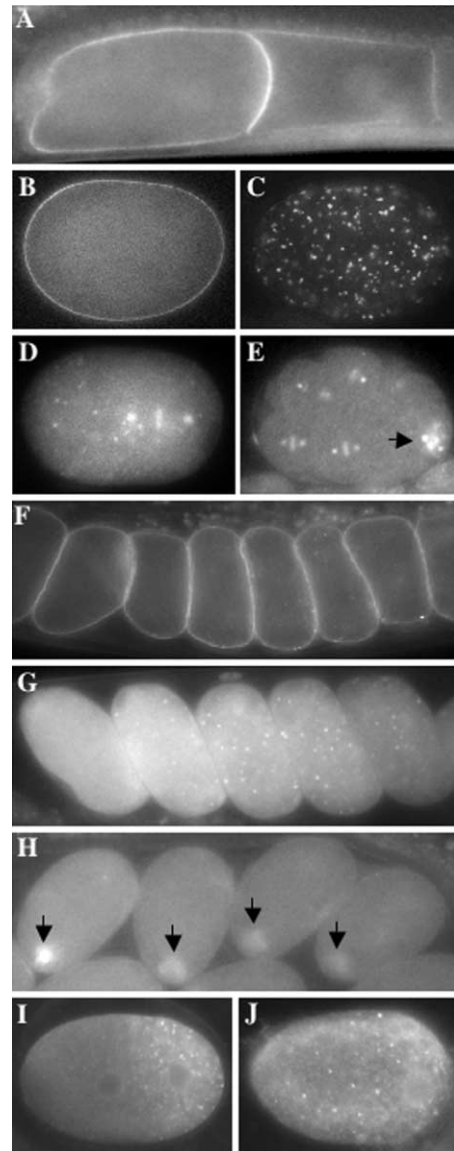


Figure 7. MBK-2 Localization Is Dynamic

(A–E) Wild-type oocytes and embryos expressing GFP:MBK-2. Thirty or more embryos were examined for each stage. (A) Oocytes. (B) Newly fertilized zygote. (C) Zygote in meiosis II. (D) Zygote in mitosis. (E) Eight-cell embryo; arrow points to P3 germline blastomere. (F–H) *mat-1(RNAi)* zygotes expressing GFP:MBK-2 (F), OMA-1:GFP (G), and GFP:MEI-1 (H). (I and J) POS-1 staining of a wild-type (I) and *mat-1(ax227)* (J) embryo.

of rescuing the embryonic lethality of *mbk-2(pk1427)* (Experimental Procedures). In oocytes and newly fertilized zygotes, GFP:MBK-2 was found predominantly at the cell periphery (cortex) in a uniform pattern (Figures 7A and 7B). In later zygotes, GFP:MBK-2 distribution changed abruptly from uniform to punctate, with GFP:MBK-2 apparently coalescing into many discrete cortical foci (Figure 7C). By mitosis, GFP:MBK-2 was found predominantly on centrosomes and chromosomes (Figure 7D),

in a pattern that persisted in all blastomeres up to at least the eight-cell stage (Figure 7E). In the germline blastomeres P2, P3, and P4, GFP:MBK-2 also appeared to associate with P granules (Figure 7E, arrow).

To determine when MBK-2 cortical foci appear after fertilization, we used a GFP:Histone H2B fusion to precisely stage embryos expressing GFP:MBK-2 (Experimental Procedures). We detected GFP:MBK-2 foci in 0/9 embryos undergoing metaphase or anaphase of meiosis I, in 3/4 embryos in telophase of meiosis I or prophase of meiosis II, and in 18/18 embryos in metaphase or anaphase of meiosis II (Experimental Procedures). After pronuclear formation, the foci disappeared quickly in a posterior-to-anterior wave. To determine whether formation of the MBK-2 foci was dependent on progression through meiosis, we examined GFP:MBK-2 in *mat-1(RNAi)* embryos. *mat-1* encodes CDC27, an APC subunit required for the metaphase-to-anaphase transition (Golden et al., 2000; Shakes et al., 2003); *mat-1(RNAi)* embryos arrest in metaphase of meiosis I. Seventy-eight percent of *mat-1(RNAi)* embryos (n = 292) maintained GFP:MBK-2 uniformly distributed at the cortex, as it is in oocytes and newly fertilized zygotes (Figure 7F). The remainder typically had fewer foci than wild-type. We conclude that redistribution of MBK-2 into cortical foci occurs just prior to the second meiotic division, and depends on progression past metaphase of meiosis I.

#### ***mbk-2*-Dependent Processes Do Not Occur in Embryos Arrested in Meiosis I**

The dramatic reorganization of MBK-2 during the meiotic divisions raised the possibility that MBK-2 becomes activated at this time, thereby triggering *mbk-2*-dependent degradation in the zygote. This hypothesis predicts that *mbk-2*-dependent events should not occur in *mat-1* embryos, which arrest prior to the appearance of MBK-2 cortical foci.

Although arrested in meiosis I, *mat-1* zygotes elaborate an A-P axis due to the lingering meiotic spindle, which mimics the polarizing function of the sperm asters (Wallenfang and Seydoux, 2000). Like *mbk-2* mutants, *mat-1* zygotes localize the PAR proteins but do not localize P granules (Wallenfang and Seydoux, 2000). *mbk-2* mutants localize PIE-1 during mitosis, but never localize POS-1 (Figures 5H and 5J). Similarly, *mat-1* zygotes localize PIE-1 (Wallenfang and Seydoux, 2000), but not POS-1 (n = 20; Figure 7J). As expected, PIE-1 segregation in *mat-1* mutants is independent of *mbk-2*: *mat-1(ax227)*; *mbk-2(RNAi)* embryos transiently localized PIE-1 as efficiently as *mat-1(ax227)* embryos (PIE-1:GFP was asymmetric in an average of 2.0 embryos per gonad in both *mat-1(ax227)* [n = 28] and *mat-1(ax227)*; *mbk-2(RNAi)* [n = 29] hermaphrodites). Like *mbk-2* embryos, *mat-1* zygotes also maintain OMA-1:GFP (Figure 7G; 34/34) and GFP:MEI-1 (Figure 7H; 40/44). The fusions persisted longer than wild-type and were eventually turned over by a mechanism independent of MBK-2 (*mat-1(ax227)*; *mbk-2(RNAi)* embryos showed the same slow loss of OMA-1:GFP and GFP:MEI-1 as *mat-1(RNAi)* embryos; data not shown). We conclude that *mbk-2*-dependent processes do not occur in *mat-1* embryos, consistent with the hypothesis

that activation of MBK-2 requires progression past meiosis I.

#### **Discussion**

In this report, we describe the embryonic functions of the DYRK kinase MBK-2. MBK-2 is required for several postfertilization events not previously suspected to be under coordinate control. These include posterior enrichment of the germ plasm in the zygote, degradation of MEI-1, MEI-2, and OMA-1 in zygotes, and degradation of PIE-1 in anterior blastomeres. MBK-2 distribution changes dramatically during the meiotic divisions, and mutants that arrest prior to this relocalization do not activate *mbk-2*-dependent processes. We propose that MBK-2 functions as a temporal regulator, which links progression through the meiotic divisions to the activation of several processes necessary to transform a symmetric egg into a patterned embryo.

#### **MBK-2 and Coordinate Activation of Maternal Protein Degradation**

A common activation step for the degradation of MEI-1/2 and PIE-1 was not expected because (1) these proteins are not related structurally or functionally, (2) are not degraded in the same pattern (MEI-1/2 in zygotes, PIE-1 in anterior cells), and (3) are not targeted by the same E3 ubiquitin ligase enzymes (DeRenzo et al., 2003; L. Pintard et al., submitted). OMA-1 turnover also appears distinct. OMA-1 is a CCCH finger protein, but unlike PIE-1, OMA-1 is degraded in all cells (Detwiler et al., 2001; Shimada et al., 2002). Furthermore, RNAi experiments indicate that OMA-1 degradation requires CUL-2, but not Elongin C or MEL-26 (the E3 subunits required for PIE-1 and MEI-1 degradation, respectively; our unpublished results). Mutations that interfere with OMA-1 degradation in embryos have been reported to delay the degradation of PIE-1 and POS-1 in somatic cells (Lin, 2003); these defects, however, are significantly weaker than the ones reported here for *mbk-2* mutants, which completely block PIE-1 degradation in somatic cells.

How then does MBK-2 participate in the activation of these apparently independent degradation pathways? MBK-2 is not required for Cyclin B degradation or cell cycle progression, and therefore is not a general activator of protein degradation or the proteasome. MBK-2 is also unlikely to be a general activator of cullins, because *cul-2* is required for *mbk-2*-independent events (Feng et al., 1999). MBK-2 must therefore act on a common component that remains to be discovered, or on each target (and/or associated proteins) individually. The CUL-1/SCF class of E3 ligases is known to require phosphorylated substrates (Skowyra et al., 1997). MBK-2 is a putative kinase; therefore, one possibility is that MBK-2 phosphorylates MEI-1/2, PIE-1, and OMA-1, and that this phosphorylation stimulates recognition by the respective E3 ligases. Whether the E3 ligases implicated in MEI-1/2 and PIE-1 degradation require phosphorylated substrates, however, is not yet known.

#### **MBK-2 and Germ Plasm Asymmetry**

MBK-2 is also required for posterior enrichment of the germ plasm in the zygote. MBK-2's effects on germ

plasm asymmetry are not secondary to its effects on MEI-1/2 and microtubule dynamics because (1) partially affected *mbk-2(RNAi)* embryos, which divide normally, still fail to segregate PIE-1 and P granules, (2) nocodazole-treated embryos and *mel-26* mutants, which exhibit microtubule defects similar to *mbk-2*, segregate PIE-1 and P granules normally, and (3) *mbk-2* does not affect polarity establishment, the only phase of the polarization process known to involve microtubules (O'Connell et al., 2000; Sadler and Shakes, 2000; Wallenfang and Seydoux, 2000). MBK-2's effects on germ plasm asymmetry are also unlikely to be secondary to the OMA-1 degradation defect, because mutations that block OMA-1 degradation in embryos do not affect germ plasm asymmetry in zygotes (Lin, 2003). Together, these observations suggest that MBK-2 regulates germ plasm asymmetry independently of its effect on other processes. One possibility is that MBK-2 affects germ plasm asymmetry by triggering the degradation of germ plasm components in the anterior half of the zygote. P granule asymmetry in the zygote is known to involve degradation or disassembly of the granules in the anterior, as well as movement of the granules along posteriorly directed cytoplasmic flows (Hird et al., 1996). Whether PIE-1 and POS-1 asymmetry in zygotes also involves localized protein degradation is not yet known. The available data, however, are consistent with this possibility. First, PIE-1 and POS-1 localizations depend on sequences in the respective ORFs, suggesting that the localization machinery acts directly on the PIE-1 and POS-1 proteins rather than the RNAs (Reese et al., 2000). Second, the same factors that regulate degradation of PIE-1 and POS-1 after the first cleavage (PAR-1, MEX-5, and MBK-2) also regulate PIE-1 and POS-1 asymmetry in the zygote (DeRenzo et al., 2003; Reese et al., 2000; Schubert et al., 2000). Third, PAR-1 contains a putative ubiquitin-associated (UBA) domain (Hofmann and Bucher, 1996). UBA domains in Rad23 inhibit the formation of substrate-linked multiubiquitin chains (Chen et al., 2001), raising the possibility that PAR-1 protects germline proteins from degradation through a similar mechanism. We propose that MBK-2 activates the degradation, or degradation competence, of several germ plasm components after meiosis, and that PAR-1 and MEX-5 subsequently restrict this degradation to the anterior. Consistent with this hypothesis, PIE-1 degradation occurs in all cells in *par-1* mutants, and this degradation is dependent on MBK-2 (Figures 6L–6N).

#### **MBK-2 and Temporal Regulation**

*mbk-2* mutants resemble embryos arrested in meiosis I (*mat-1* mutants), which also localize PAR proteins, but do not localize P granules and POS-1, and do not degrade MEI-1 and OMA-1. Unlike *mat-1* mutants, however, *mbk-2* mutants proceed through meiosis and on to mitosis as in wild-type. These observations indicate that progression through the meiotic divisions, while not dependent on *mbk-2*, is required to activate *mbk-2*-dependent processes.

MBK-2 localization changes dramatically during the transition from meiosis I to meiosis II, suggesting that MBK-2 itself is activated during the meiotic divisions. We propose that the transition from meiosis I to meiosis

II activates MBK-2, which in turn stimulates the degradation, or degradation competence, of several maternal proteins. Why activate MBK-2 at this time? OMA-1 and MEI-1/2 are required for oocyte maturation and for the meiotic divisions, respectively, so it is important to degrade these proteins after but not before the meiotic divisions. Polarization of the A-P axis in wild-type embryos requires the sperm asters, which form after the meiotic divisions. Linking MBK-2 activation to meiosis, therefore, ensures that polarity cues are in place by the time germ plasm degradation begins.

A link between progression through meiosis and developmental events has also been observed in *Drosophila*. In *Drosophila* oocytes, progression through meiotic prophase is required for efficient translation of *gurken*, a TGF- $\alpha$  signal essential for the establishment of anteroposterior and dorsoventral axes (Ghabrial et al., 1998; Ghabrial and Schupbach, 1999). Mutations in DNA repair genes that lead to a checkpoint arrest during meiotic prophase impair *gurken* translation. Similarly, in newly fertilized embryos, completion of the meiotic divisions is essential to activate the translation of several maternal mRNAs. Mutations that arrest embryos in metaphase of meiosis II block translation of *bicoid*, a transcription factor essential for anteroposterior patterning (Chen et al., 2000; Chu et al., 2001). In both cases, it is not known whether cell cycle regulators act directly on developmental targets or function through intermediates that are cell cycle regulated but are themselves not required for cell cycle progression. Our findings here suggest that MBK-2 is such an intermediate, linking progression through the meiotic divisions to the degradation of several maternal proteins.

#### **MBK-2 and the DYRK Family**

MBK-2 belongs to the DYRK family of dual-specificity protein kinases. This family comprises two main subgroups. The first includes *Drosophila minibrain*, human DYRK1A and DYRK1B, and *C. elegans mbk-1*. *minibrain* is required for postembryonic neurogenesis in the *Drosophila* brain (Tejedor et al., 1995). Human DYRK1A is located in the "Down's syndrome critical region" of chromosome 21 (Guimera et al., 1996; Kentrup et al., 1996), and overexpression in mice has been shown to result in cognitive deficits and motor abnormalities (Altafaj et al., 2001). Similarly, overexpression of *mbk-1* in worms leads to chemotaxis and olfaction defects (Raich et al., 2003). These findings suggest a common role for the DYRK1 subgroup in neuronal development and/or function. The cellular function for this class, however, remains unknown. MBK-2 belongs to the second subgroup, which include three human proteins of unknown function (DYRK2, DYRK3, and DYRK4), *Drosophila* DYRK2, and *S. pombe* Pom1p. Remarkably, several parallels can be drawn between MBK-2 and Pom1p. Like MBK-2, Pom1p regulates both cell polarity and cell division (Bahler and Pringle, 1998). *S. pombe* cells divide and grow in a stereotypical pattern: cells first initiate growth at their "old" end (the end present in the mother cell prior to division), switch to bipolar growth upon entering the G2 phase, and divide by medial fission to generate equal-sized daughter cells. *pom1* mutants exhibit defects in each of these steps: they randomly

begin to elongate at either end, rarely switch to bipolar growth, and frequently misplace and/or misorient their division septa, leading to cells with uneven shapes. How Pom1p regulates these processes is not yet known, but like MBK-2, Pom1p localizes to the mitotic spindle and has been proposed to influence microtubule dynamics (Bahler and Pringle, 1998). Pom1p kinase activity oscillates with the cell cycle (Bahler and Nurse, 2001), with the highest levels occurring during the time of bipolar growth and cell division, suggesting that Pom1p activation is what triggers these processes. Thus, as we propose here for MBK-2, Pom1p activity is cell cycle regulated and may function to coordinate certain developmental events (i.e., switch to bipolar growth) with the proper phase of the cell cycle.

Our findings suggest that MBK-2 functions, directly or indirectly, by stimulating the degradation of maternal proteins. Whether Pom1p also regulates protein turnover is not yet known. A recent study, however, suggests that another member of the family, *DYRK1B*, may have a similar function. Overexpression of *DYRK1B* in colon carcinoma cells leads to rapid turnover of the cdk inhibitor p27(kip1) and the G1 Cyclin D1 (Ewton et al., 2003). An intriguing possibility is that DYRK kinases have evolved to target different proteins for degradation in different cell types. Continued analysis of DYRK family members in different systems will be essential to unravel the core functions unique to this family.

#### Experimental Procedures

##### Nematode Strains

*C. elegans* strains were derived from the wild-type Bristol strain N2 and maintained at 25°C using standard procedures (Brenner, 1974). See Table 1 for a description of strains used in this study.

##### RNA-Mediated Interference and Screen

Double-stranded RNAs (dsRNAs) corresponding to 733 germline-enriched genes (Reinke et al., 2000) were synthesized in two steps. First, ~1 kb of genomic sequence was PCR amplified for each gene using gene-specific primers carrying T7 promoter sequences (Reinke et al., 2000). Second, each PCR product was transcribed in both orientations in a single in vitro transcription reaction (Promega RiboMAX T7 kit). The resulting dsRNAs were injected in pools of four into young adult JH227 hermaphrodites, which express PIE-1:GFP. Injected hermaphrodites were recovered overnight at 20°C, shifted to 25°C for ~8 hr, and screened for embryos with abnormal PIE-1:GFP patterns. dsRNAs from positive pools were reinjected individually to identify the gene of interest. The same approach was used to generate and test dsRNAs corresponding to specific exons in *mbk-2*.

All other RNAi experiments in this study were performed using the feeding method (Timmons et al., 2001). For *mbk-2(RNAi)*, feeding for 30–34 hr at 25°C resulted in phenotypes identical to those observed in *mbk-2(pk1427)* embryos. Feeding for 15–29 hr often resulted in partially affected embryos that completed several cleavages, but still failed to segregate germ plasm and to rapidly degrade OMA-1.

##### Time-Lapse Microscopy and Phenotypic Analysis

Time-lapse microscopy was performed as described in Cuenca et al. (2003). Supplemental Movies 1, 6, 11, 12, 13, 15, 17, 18, 19, and 22 are included in Supplemental Data at <http://www.developmentalcell.com/cgi/content/full/5/3/451/DC1>. All movies can be viewed at [ftp://ftp.wormbase.org/pub/wormbase/datasets/pellettieri\\_2003](ftp://ftp.wormbase.org/pub/wormbase/datasets/pellettieri_2003). We typically began our time-lapse analysis after meiosis, around the time that the maternal and paternal pronuclei first appear. Initially, the paternal pronucleus remains close to the cortex; cytoplasmic flow is strongest during that time and was easily detected in 8/8

Table 1. Strains Used in This Study

Name	Description	Genotype	Reference
JH227	$P_{pie-1}$ :PIE-1:GFP	<i>axEx73[pJH3.92; pRF4]</i>	Reese et al., 2000
JH1448	$P_{pie-1}$ :GFP:MEX-5	<i>axEx1125[pKR2.04; pRF4]</i>	Cuenca et al., 2003
KK866	$P_{pie-1}$ :GFP:PAR-2	<i>itIs153[pMW1.03; pRF4]</i>	Wallenfang and Seydoux, 2000
AZ212	$P_{pie-1}$ :GFP:Histone H2B	<i>unc-119(ed3);ruIS32 [pAZ 132]</i>	Prattis et al., 2001
JH1514	$P_{pie-1}$ :GFP:PGL-1	<i>unc-119(ed3); isax 1138[pID11.01]</i>	I. D'Agostino and G.S., unpublished
JH1276	$P_{pie-1}$ :GFP:PIE-1 <sup>271</sup>	<i>axEx1070[pKR1.58; pRF4]</i>	Reese et al., 2000
JH1414	<i>mat-1</i> ; $P_{pie-1}$ :PIE-1:GFP	<i>mat-1(ax227); axEx73[pJH3.92; pRF4]</i>	Wallenfang and Seydoux, 2000
KK292	<i>par-1</i>	<i>rol-4(sc8) par-1(it51)/DnT1 V</i>	Guo and Kemphues, 1995
WH204	$P_{pie-1}$ :GFP:β-Tubulin	<i>oJIs1[pJH4.66 w/unc-119 inserted at NaeI]</i>	Strome et al., 2001
EU1065	$P_{pie-1}$ :GFP:MEI-1	<i>unc-119(ed3); [P<sub>pie-1</sub>:GFP:MEI-1]</i>	Prattard et al., 2003
ET113	$P_{pie-1}$ :GFP:Cyclin B (cyb-1)	<i>unc-119(ed3); ekIs2[pD3.01b/cyb-1]</i>	E. Kipreos, personal communication
TX189	$P_{omb-1}$ :OMA-1:GFP	<i>unc-119(ed3); tels1[pRL475 + pPDM016]</i>	Lin, 2003
JH1573	<i>dpy-4 mbk-2/nT1</i>	<i>dpy-4(e1166) mbk-2(pk1427)/nT1</i>	This study
JH1572	$P_{pie-1}$ :GFP:MBK-2 (Inj.)	<i>axEx1139[pJP1.01;pRF4]</i>	This study
JH1576	$P_{pie-1}$ :GFP:MBK-2 (Bomb.)	<i>axIs1140[pJP1.02]</i>	This study
JH1575	$P_{pie-1}$ :GFP:MBK-2; $P_{pie-1}$ :GFP:Histone H2B	<i>axEx1139[pJP1.01;pRF4]; ruIs32[pAZ 132]</i>	This study
JH1593	<i>unc-24 mbk-2/nT1</i> ; $P_{pie-1}$ :GFP:Histone H2B	<i>unc-24(e1172) mbk-2(pk1427)/nT1; ruIs32[pAZ 132]</i>	This study
JH1574	<i>mat-1</i> ; $P_{omb-1}$ :OMA-1:GFP	<i>mat-1(ax227); tels1[pRL475 + pPDM016]</i>	This study

*mbk-2(pk1427)* zygotes examined during that period. All *mbk-2(pk1427)* zygotes (13/13) examined during pronuclear migration showed an expanding smooth zone near the sperm pronucleus (posterior) and a receding contractile zone in the anterior, culminating in pseudocleavage. These characteristics are consistent with normal polarization of the cortex by the sperm asters (Cuenca et al., 2003). All *mbk-2(pk1427)* zygotes (18/18) had a single maternal pronucleus and an osmotically resistant eggshell, and 16/18 had at least one visible polar body, consistent with normal meiosis. Examination of *mbk-2(pk1427)* zygotes expressing GFP:Histone H2B confirmed that chromosomes adopt normal configurations during both meiotic divisions (6/6 meiosis I embryos, and 9/9 meiosis II embryos examined). *mbk-2(pk1427)* hermaphrodites never had more than one meiotic embryo per gonad arm ( $n = 42$  gonad arms), as in wild-type ( $n = 63$  gonad arms), but in clear contrast to meiotic mutants, which accumulate several meiotic embryos in the uterus (Shakes et al., 2003).

#### GFP:MBK-2

A genomic fragment spanning the ORF in *mbk-2c* (Figure 1A) was cloned into two vectors, pJH4.52 and pID3.01, to create amino-terminal GFP fusions. These vectors utilize *pie-1* 5' and 3' UTR sequences to drive expression of the transgene in the maternal germline. GFP lines were created by the complex array method (pJH4.52; Kelly et al., 1997) or by the microparticle bombardment method (pID3.01; Pratis et al., 2001). Several independent lines were established using each technique. Although expression levels varied from line to line, all lines showed the same overall distribution of GFP:MBK-2. Crossing of JH1572 (GFP:MBK-2) into JH1573 (*dpy-4(e1166) mbk-2(pk1427)/nT1*) rescued the maternal-effect embryonic lethality of *mbk-2(pk1427)* homozygotes: *dpy-4(e1166) mbk-2(pk1427)* hermaphrodites laid dead embryos, whereas GFP:MBK-2; *dpy-4(e1166) mbk-2(pk1427)* hermaphrodites were fertile for 15+ generations. We crossed JH1572 to AZ212 to obtain JH1575, which coexpresses GFP:MBK-2 and GFP:Histone H2B. Chromosome morphology and number of polar bodies (zero during meiosis I, one during meiosis II) were used to determine meiotic stages as in Golden et al. (2000).

#### Immunofluorescence Staining

Immunofluorescence staining was performed as described in Guo and Kempfues (1995). Embryos were fixed in  $-20^{\circ}\text{C}$  methanol (15 min) followed by  $-20^{\circ}\text{C}$  acetone (10 min) for staining with anti-PIE-1 (Tenenhaus et al., 1998), anti-POS-1 (Tabara et al., 1999), anti-P granules (Strome and Wood, 1983), anti-PAR-1 (Guo and Kempfues, 1995), anti-PAR-3 (Etemad-Moghadam et al., 1995), anti-Tubulin (DM1A; Sigma), and anti-MEI-2 (Srayko et al., 2000). Embryos were fixed in  $-20^{\circ}\text{C}$  methanol (5 min) followed by room temperature formaldehyde solution ( $1 \times$  PBS, 1.6 mM  $\text{MgSO}_4$ , 0.8 mM EGTA, 3.7% formaldehyde; 30 min) for staining with anti-MEX-5 (Schubert et al., 2000).

#### Acknowledgments

We thank Y. Kohara for cDNAs, W. Raich and O. Hobert for *mbk-2(pk1427)*, R. Lin for OMA-1:GFP, T. Kurz and B. Bowerman for GFP:MEI-1, E. Kipreos for GFP:Cyclin B, the *Caenorhabditis* Genetics Center (funded by the NIH Center for Research Resources) for strains, and R. Lin, C. Shelton, B. Bowerman, M. Peter, E. Kipreos, and O. Hobert for sharing unpublished data. We also thank K. O'Connell, A. Golden, and T. Schedl for enlightening discussions and suggestions, and B. Bowerman and T. Schedl for critical reading of the manuscript. This work was supported by NIH RO1 grant M400-150-2298 (G.S.), and by NIH training grant CA 09139 (J.P.).

Received: March 26, 2003

Revised: May 28, 2003

Accepted: June 16, 2003

Published: September 8, 2003

#### References

Altajaj, X., Dierssen, M., Baamonde, C., Marti, E., Visa, J., Guimera, J., Oset, M., Gonzalez, J.R., Florez, J., Fillat, C., and Estivill, X. (2001).

Neurodevelopmental delay, motor abnormalities and cognitive deficits in transgenic mice overexpressing Dyrk1A (minibrain), a murine model of Down's syndrome. *Mol. Genet.* **10**, 1915–1923.

Bahler, J., and Nurse, P. (2001). Fission yeast Pom1p kinase activity is cell cycle regulated and essential for cellular symmetry during growth and division. *EMBO J.* **20**, 1064–1073.

Bahler, J., and Pringle, J.R. (1998). Pom1p, a fission yeast protein kinase that provides positional information for both polarized growth and cytokinesis. *Genes Dev.* **12**, 1356–1370.

Becker, W., and Joost, H.G. (1999). Structural and functional characteristics of Dyrk, a novel subfamily of protein kinases with dual specificity. *Prog. Nucleic Acid Res. Mol. Biol.* **62**, 1–17.

Becker, W., Weber, Y., Wetzel, K., Eirnbter, K., Tejedor, F.J., and Joost, H.G. (1998). Sequence characteristics, subcellular localization, and substrate specificity of DYRK-related kinases, a novel family of dual specificity protein kinases. *J. Biol. Chem.* **273**, 25893–25902.

Boyd, L., Guo, S., Levitan, D., Stinchcomb, D.T., and Kempfues, K.J. (1996). PAR-2 is asymmetrically distributed and promotes association of P granules and PAR-1 with the cortex in *C. elegans* embryos. *Development* **122**, 3075–3084.

Brenner, S. (1974). The genetics of *Caenorhabditis elegans*. *Genetics* **77**, 71–94.

Chen, B., Harms, E., Chu, T., Henrion, G., and Strickland, S. (2000). Completion of meiosis in *Drosophila* oocytes requires transcriptional control by grauzone, a new zinc finger protein. *Development* **127**, 1243–1251.

Chen, L., Shinde, U., Ortolan, T.G., and Madura, K. (2001). Ubiquitin-associated (UBA) domains in Rad23 bind ubiquitin and promote inhibition of multi-ubiquitin chain assembly. *EMBO Rep.* **2**, 933–938.

Chu, T., Henrion, G., Haegeli, V., and Strickland, S. (2001). Cortex, a *Drosophila* gene required to complete oocyte meiosis, is a member of the Cdc20/fizzy protein family. *Genesis* **29**, 141–152.

Cuenca, A.A., Schetter, A., Aceto, D., Kempfues, K., and Seydoux, G. (2003). Polarization of the *C. elegans* zygote proceeds via distinct establishment and maintenance phases. *Development* **130**, 1255–1265.

DeRenzo, C., Reese, K., and Seydoux, G. (2003). Exclusion of germ plasm proteins from somatic lineages by cullin-dependent degradation. *Nature* **424**, 685–689. Published online July 23, 2003. 10.1038/nature01887

Detwiler, M.R., Reuben, M., Li, X., Rogers, E., and Lin, R. (2001). Two zinc finger proteins, OMA-1 and OMA-2, are redundantly required for oocyte maturation in *C. elegans*. *Dev. Cell* **1**, 187–199.

Dow, M.R., and Mains, P.E. (1998). Genetic and molecular characterization of the *Caenorhabditis elegans* gene, mei-26, a postmeiotic negative regulator of mei-1, a meiotic-specific spindle component. *Genetics* **150**, 119–128.

Etemad-Moghadam, B., Guo, S., and Kempfues, K.J. (1995). Asymmetrically distributed PAR-3 protein contributes to cell polarity and spindle alignment in early *C. elegans* embryos. *Cell* **83**, 743–752.

Ewton, D.Z., Lee, K., Deng, X., Lim, S., and Friedman, E. (2003). Rapid turnover of cell-cycle regulators found in Mirk/dyrk1B transfectants. *Int. J. Cancer* **103**, 21–28.

Feng, H., Zhong, W., Punkosdy, G., Gu, S., Zhou, L., Seabolt, E.K., and Kipreos, E.T. (1999). CUL-2 is required for the G1-to-S-phase transition and mitotic chromosome condensation in *Caenorhabditis elegans*. *Nat. Cell Biol.* **1**, 486–492.

Garrett, S., and Broach, J. (1989). Loss of Ras activity in *Saccharomyces cerevisiae* is suppressed by disruptions of a new kinase gene, YAK1, whose product may act downstream of the cAMP-dependent protein kinase. *Genes Dev.* **3**, 1336–1348.

Ghabrial, A., and Schupbach, T. (1999). Activation of a meiotic checkpoint regulates translation of Gurken during *Drosophila* oogenesis. *Nat. Cell Biol.* **1**, 354–357.

Ghabrial, A., Ray, R.P., and Schupbach, T. (1998). okra and spindle-B encode components of the RAD52 DNA repair pathway and affect meiosis and patterning in *Drosophila* oogenesis. *Genes Dev.* **12**, 2711–2723.

- Golden, A., Sadler, P.L., Wallenfang, M.R., Schumacher, J.M., Hamill, D.R., Bates, G., Bowerman, B., Seydoux, G., and Shakes, D.C. (2000). Metaphase to anaphase (mat) transition-defective mutants in *Caenorhabditis elegans*. *J. Cell Biol.* **151**, 1469–1482.
- Guimera, J., Casas, C., Pucharcos, C., Solans, A., Domenech, A., Planas, A.M., Ashley, J., Lovett, M., Estivill, X., and Pritchard, M.A. (1996). A human homologue of *Drosophila* minibrain (MNB) is expressed in the neuronal regions affected in Down syndrome and maps to the critical region. *Hum. Mol. Genet.* **5**, 1305–1310.
- Guo, S., and Kemphues, K.J. (1995). par-1, a gene required for establishing polarity in *C. elegans* embryos, encodes a putative Ser/Thr kinase that is asymmetrically distributed. *Cell* **81**, 611–620.
- Hird, S.N., Paulsen, J.E., and Strome, S. (1996). Segregation of germ granules in living *Caenorhabditis elegans* embryos: cell-type-specific mechanisms for cytoplasmic localisation. *Development* **122**, 1303–1312.
- Hofmann, K., and Bucher, P. (1996). The UBA domain: a sequence motif present in multiple enzyme classes of the ubiquitination pathway. *Trends Biochem. Sci.* **21**, 172–173.
- Kelly, W.G., Xu, S., Montgomery, M.K., and Fire, A. (1997). Distinct requirements for somatic and germline expression of a generally expressed *Caenorhabditis elegans* gene. *Genetics* **146**, 227–238.
- Kentrup, H., Becker, W., Heukelbach, J., Wilmes, A., Schurmann, A., Huppertz, C., Kainulainen, H., and Joost, H.G. (1996). Dyrk, a dual specificity protein kinase with unique structural features whose activity is dependent on tyrosine residues between subdomains VII and VIII. *J. Biol. Chem.* **271**, 3488–3495.
- Kurz, T., Pintard, L., Willis, J.H., Hamill, D.R., Gonczy, P., Peter, M., and Bowerman, B. (2002). Cytoskeletal regulation by the Nedd8 ubiquitin-like protein modification pathway. *Science* **295**, 1294–1298.
- Lin, R. (2003). A gain-of-function mutation in oma-1, a *C. elegans* gene required for oocyte maturation, results in delayed degradation of maternal proteins and embryonic lethality. *Development*, in press.
- Lyczak, R., Gomes, J.E., and Bowerman, B. (2002). Heads or tails: cell polarity and axis formation in the early *Caenorhabditis elegans* embryo. *Dev. Cell* **3**, 157–166.
- McNally, F.J., and Vale, R.D. (1993). Identification of katanin, an ATPase that severs and disassembles stable microtubules. *Cell* **75**, 419–429.
- Mendez, R., and Richter, J.D. (2001). Translational control by CPEB: a means to the end. *Nat. Rev. Mol. Cell Biol.* **2**, 521–529.
- O'Connell, K.F., Maxwell, K.N., and White, J.G. (2000). The spd-2 gene is required for polarization of the anteroposterior axis and formation of the sperm asters in the *Caenorhabditis elegans* zygote. *Dev. Biol.* **222**, 55–70.
- Pintard, L., Kurz, T., Glaser, S., Willis, J.H., Peter, M., and Bowerman, B. (2003). Neddylation and deneddylation of CUL-3 is required to target MEI-1/katanin for degradation at the meiosis-to-mitosis transition in *C. elegans*. *Curr. Biol.* **13**, 911–921.
- Praitis, V., Casey, E., Collar, D., and Austin, J. (2001). Creation of low-copy integrated transgenic lines in *Caenorhabditis elegans*. *Genetics* **157**, 1217–1226.
- Raich, W.B., Moorman, C., Laceyfield, C.O., Lehrer, J., Bartsch, D., Plasterk, R.H., Kandel, E.R., and Hobert, O. (2003). Characterization of *Caenorhabditis elegans* homologs of the Down syndrome candidate gene DYRK1A. *Genetics* **163**, 571–580.
- Reese, K.J., Dunn, M.A., Waddle, J.A., and Seydoux, G. (2000). Asymmetric segregation of PIE-1 in *C. elegans* is mediated by two complementary mechanisms that act through separate PIE-1 protein domains. *Mol. Cell* **6**, 445–455.
- Reinke, V., Smith, H.E., Nance, J., Wang, J., Van Doren, C., Begley, R., Jones, S.J., Davis, E.B., Scherer, S., Ward, S., and Kim, S.K. (2000). A global profile of germline gene expression in *C. elegans*. *Mol. Cell* **6**, 605–616.
- Sadler, P.L., and Shakes, D.C. (2000). Anucleate *Caenorhabditis elegans* sperm can crawl, fertilize oocytes and direct anterior-posterior polarization of the 1-cell embryo. *Development* **127**, 355–366.
- Schubert, C.M., Lin, R., de Vries, C.J., Plasterk, R.H., and Priess, J.R. (2000). MEX-5 and MEX-6 function to establish soma/germline asymmetry in early *C. elegans* embryos. *Mol. Cell* **5**, 671–682.
- Shakes, D.C., Sadler, P.L., Schumacher, J.M., Abdolrasulnia, M., and Golden, A. (2003). Developmental defects observed in hypomorphic anaphase-promoting complex mutants are linked to cell cycle abnormalities. *Development* **130**, 1605–1620.
- Shimada, M., Kawahara, H., and Doi, H. (2002). Novel family of CCCH-type zinc-finger proteins, MOE-1, -2 and -3, participates in *C. elegans* oocyte maturation. *Genes Cells* **7**, 933–947.
- Skowyrza, D., Craig, K.L., Tyers, M., Elledge, S.J., and Harper, J.W. (1997). F-box proteins are receptors that recruit phosphorylated substrates to the SCF ubiquitin-ligase complex. *Cell* **91**, 209–219.
- Srayko, M., Buster, D.W., Bazirgan, O.A., McNally, F.J., and Mains, P.E. (2000). MEI-1/MEI-2 katanin-like microtubule severing activity is required for *Caenorhabditis elegans* meiosis. *Genes Dev.* **14**, 1072–1084.
- Strome, S., and Wood, W.B. (1983). Generation of asymmetry and segregation of germ-line granules in early *C. elegans* embryos. *Cell* **35**, 15–25.
- Strome, S., Powers, J., Dunn, M., Reese, K., Malone, C.J., White, J., Seydoux, G., and Saxton, W. (2001). Spindle dynamics and the role of  $\gamma$ -tubulin in early *Caenorhabditis elegans* embryos. *Mol. Biol. Cell* **12**, 1751–1764.
- Suzumori, N., Burns, K.H., Yan, W., and Matzuk, M.M. (2003). RFPL4 interacts with oocyte proteins of the ubiquitin-proteasome degradation pathway. *Proc. Natl. Acad. Sci. USA* **100**, 550–555.
- Tabara, H., Hill, R.J., Mello, C.C., Priess, J.R., and Kohara, Y. (1999). pos-1 encodes a cytoplasmic zinc-finger protein essential for germline specification in *C. elegans*. *Development* **126**, 1–11.
- Tejedor, F., Zhu, X.R., Kaltenbach, E., Ackermann, A., Baumann, A., Canal, I., Heisenberg, M., Fischbach, K.F., and Pongs, O. (1995). minibrain: a new protein kinase family involved in postembryonic neurogenesis in *Drosophila*. *Neuron* **14**, 287–301.
- Tenenhaus, C., Schubert, C., and Seydoux, G. (1998). Genetic requirements for PIE-1 localization and inhibition of gene expression in the embryonic germ lineage of *Caenorhabditis elegans*. *Dev. Biol.* **200**, 212–224.
- Timmons, L., Court, D.L., and Fire, A. (2001). Ingestion of bacterially expressed dsRNAs can produce specific and potent genetic interference in *Caenorhabditis elegans*. *Gene* **263**, 103–112.
- Wallenfang, M.R., and Seydoux, G. (2000). Polarization of the anterior-posterior axis of *C. elegans* is a microtubule-directed process. *Nature* **408**, 89–92.